AD-A276 715

OFFICE OF NAVAL RESEARCH

Contract No. N00014-91-J-1409

Technical Report No. 147

Scanning Tunneling Microscopy and Infrared Spectroscopy as Combined In-Situ Probes of Electrochemical Adlayer Structure: Cyanide on Pt(111)

DTIC
ELECTE
MAR 10 1994
S D
F

by

Christopher Stuhlmann, Ignacio Villegas, and Michael J. Weaver

Prepared for Publication

in

Chemical Physics Letters

94-07827

Department of Chemistry

Purdue University

West Lafayette, Indiana 47907-1393

February 1994

Reproduction in whole, or in part, is permitted for any purpose of the United States Government.

* This document has been approved for public release and sale; its distribution is unlimited.

94 3 9 077

Best
Available
Copy

Abstract

The spatial structure of irreversibly adsorbed cyanide adlayers on a Pt(111) electrode is deduced by means of in-situ scanning tunneling microscopy (STM) combined with infrared reflection-absorption spectroscopy (IRAS). The latter data suggests atop-like Pt-CN coordination. The STM images display a (2/3 × 2/3)R30°-7CN structure, with cyanides bound in symmetric atop sites surrounded by hexagonal "clusters" of CN, likely bound in near-atop sites. This arrangement, stable over the applied potential range -0.5 to 0 V vs SCE, gives way to a (2 × 2) structure and disordered adlayers at lower potentials. These findings are compared with previous structural information deduced from ex-situ electron diffraction.

Accesion For
NTIS CRA&I
DTIC TAB
Unannounced
Justification
By
Distribution /
Availability Codes
Dist | Avail and / or Special
A-1

1. Introduction

As for metal surfaces in ultrahigh vacuum (uhv) environments, the elucidation of adlayer structures at metal-solution (i.e. electrochemical) interfaces is of central fundamental interest. Until recently, such information was obtainable only by means of ex-situ tactics, involving transferral of the electrode into uhv followed by characterization using low energy electron diffraction (LEED) and other methods[1]. However, the advent of an increasing range of microscopic and spectroscopic techniques applicable directly to electrochemical interfaces is now enabling detailed in-situ adlayer structural information to be extracted for a significant range of systems[2].

Although beset by some limitations, scanning tunneling microscopy (STM) provides an especially direct probe of real-space surface structure. An increasing number of recent reports attest to the ability of STM to yield such information for adlayers as well as the metal substrate at electrochemical interfaces with true atomic resolution[2]. For molecular adsorbates, the opportunity arises to supplement this real-space structural information with insight into adlayer-surface bonding as can be provided in suitable cases by infrared reflection-absorption spectroscopy (IRAS). This combined in-situ STM/IRAS tactic can allow the nature of the adsorbate bonding sites to be deduced together with the adlayer packing arrangement. A related approach, combining LEED with vibrational spectral information from either IRAS or electron energy loss spectroscopy (EELS), has been used to elucidate adlayer structure in uhv[3].

The first combined STM/IRAS study for an electrochemical system, reported from this laboratory, involved deducing potential-dependent adlayer structures for carbon monoxide on Rh(111) in aqueous solution[4]. Subsequent reports of adlayer structures deduced in this manner involve CO on Rh(110)[5] and Pt(111)[6]. A related adsorbate also suitable for such analyses is cyanide.

Hubbard and coworkers showed by LEED that ordered cyanide adlayers could be formed on Pt(111) in cyanide-containing solution that readily withstand electrode emersion into uhv[7,8]. Korzeniewski and coworkers have utilized a similar emersion tactic to obtain in-situ infrared spectra for predosed cyanide adlayers on polycrystalline and ordered low-index Pt surfaces in aqueous solution[9,10].

We describe here a combined in-situ STM/IRAS study of irreversibly adsorbed cyanide adlayers on Pt(111). While consistent with ex-situ LEED data[7,8], the derived real-space adlattices differ significantly from the structures suggested earlier. We also note briefly the nature of cyanide adsorption on Pt(100) as deduced using the in-situ STM/IRAS approach.

2. Experimental

Cyanide adlayers were prepared using the same procedure for both IRAS and STM experiments. The Pt(111) crystal was annealed to yellowness in a hydrogen-air flame, then cooled in iodine vapor, yielding an iodine-protected surface. The iodine was replaced by CO in an electrochemical cell containing CO-saturated 0.1 M $HClO_4$, the adlayer then being removed by electrochemical oxidation in CO-free $HClO_4$[11]. The CN^- was adsorbed in a separate electrochemical cell containing 1 mM NaCN and 0.1 M $NaClO_4$ by transferring the Pt(111) surface (protected by a drop of water) into this solution at a controlled "dosing potential". After 3 min, the sample was transferred either to the IRAS or the STM cell containing 0.1 M $NaClO_4$ adjusted to a pH between 10 and 11 with NaOH (cf. ref. 10). No significant voltammetric current was observed for the CN^--coated surface between -0.65 V and 0.30 V vs. SCE, indicating the formation of a passivation layer.

The FTIR spectrometer used was an IBM (Bruker) IR-98-4A vacuum instrument with a Globar light source and an MCT detector. The IRAS arrangement is described elsewhere[12]. The scanning tunneling microscope was a commercial

Nanoscope II instrument (Digital Instruments, Inc.) with a bipotentiostat for in-situ electrochemical STM, utilizing Pt/Ir tips electrochemically etched in near-saturated $CaCl_2$ and coated with a thermosetting plastic[13]. The quasi-reference electrode was a gold wire.

The Pt(111) single crystals were purchased from the Materials Preparation Facility at Cornell University. The misorientation was below 1°, as verified by X-ray backscattering. All chemicals used were reagent grade or better. All potentials are quoted vs. the saturated calomel electrode (SCE) and all measurements were made at 23 ± 1°C.

3. Results and Discussion

A typical series of potential-difference infrared (PDIR) spectra, recorded for a CN^--covered surface, is displayed in Fig. 1. The immersion potential in the cyanide dosing cell was -0.6 V. The spectra were obtained by alternating the electrode potential periodically between a suitably different ("reference" and "sample") pair of electrode potentials until the desired number (typically 500-1000) of appropriately coadded interferometer scans was accumulated. This procedure yields a bipolar band around 2100 cm^{-1} (Fig. 1) , assigned to the C-N stretching vibration of adsorbed CN^-. As is commonly observed, the double-sided character of the band indicates the presence of adsorbed CN^- at both the lower and upper potentials. As displayed in Fig. 1, the usual potential-induced ("Stark tuning") frequency shift of the vibrational band yields apparent negative and positive adsorbances at the lower and upper potentials, respectively. The spectra in Fig. 1 were recorded with a constant lower potential of -0.5 V, while the upper potential is altered as indicated: hence, the negative-going peak remains at a fixed position while the frequency of the positive-going peak upshifts with increasing potential.

Such data enable the C-N stretching frequency, ν_{CN}, to be obtained as a

function of the electrode potential, E, by suitable variations in the lower as well as upper modulation potentials, keeping the difference in these values sufficiently large (> 0.2 to 0.3 V) so to minimize the mutual interference between the positive- and negative-going bipolar band components. At sample potentials more positive than 0.3 V, partial oxidation of the cyanide adlayer to CO_2 commences, as evidenced by the appearance of the asymmetric CO_2 stretching vibration at 2343 cm^{-1}. While the observed electrooxidation of adsorbed CN^- to CO_2 on Pt(111) is in qualitative agreement with ref. 10, we typically observed only partial electrooxidative removal in the present experiments under potential-step conditions. (This circumstance obliged us to utilize here the potential-modulation procedure to obtain bipolar spectra, rather than the (simpler) unipolar bands observed when complete electrooxidation adsorbate removal can be achieved, as for CO on Pt(111) for example[12]. We were therefore also unable to quantify the cyanide coverage from the spectroelectrochemical assay of the CO_2 product.)

Despite these limitations, PDIR spectra such as those in Fig. 1 show clearly the presence of only a single ν_{CN} feature that upshifts in frequency in roughly linear fashion with increasing E, yielding a ν_{CN}-E slope of about 50–55 cm^{-1}. Some dependence of the ν_{CN} frequencies upon the CN^- dosing potential, E_{dos}, was observed: as E_{dos} was increased from –0.6 to 0 V the ν_{CN} frequencies at the highest applied potentials, 0.2 to 0.3 V, were upshifted by 5–10 cm^{-1}, although the values at the lowest applied potentials were virtually unaffected. The band intensities, however, were largely unaffected under these conditions. Some PDIR experiments were performed where the I-coated Pt(111) surface formed by the annealing–cooling procedure was dosed directly with cyanide rather than being subjected to the intermediate CO-dosing/electrooxidation step to remove separately the iodide (vide supra). Not unexpectedly, the ν_{CN} frequencies and

band intensities decrease progressively for dosing potentials above −0.4 V, consistent with an increasingly incomplete removal of iodide by cyanide under these conditions.

As noted recently by Kim and Korzeniewski[10], the observation of a single ν_{CN} feature at ca 2090–2130 cm^{-1} is apparently indicative of the presence of a largely uniform CN surface binding via the carbon atom, probably in an atop geometry (i.e. involving an single Pt atom). The deduction of a particular binding geometry from the infrared frequencies alone is, however, less reliable than for the better-understood case of CO. An additional means of binding-site diagnosis utilized here involves examining the effects of predosing bismuth adatoms on Pt(111) upon the cyanide infrared spectra. This tactic has been examined previously for the adsorption of CO on Pt(111) and (100) in aqueous media[14]. The presence of saturated Bi adlayers was found to remove selectively the bridging or threefold hollow CO which is otherwise prevalent at these interfaces: this finding is consistent with the anticipated binding of the irreversibly bound Bi atoms in multifold adsorption geometries, thereby denying access of the postdosed CO to such sites[6,14].

Figure 2A shows the result of applying this procedure to the Pt(111)/CN system. The upper PDIR spectrum (referring to reference and sample potentials of −0.3 V and 0.1 V, respectively) was obtained after dosing a clean Pt(111) surface with cyanide at −0.1 V, whereas the lower spectrum was obtained similarly, but after predosing a saturated Bi layer (coverage ~ 0.3) as outlined in ref. 14. While the lower spectrum displays slightly lower intensities and downshifted ν_{CN} frequencies (the latter probably being due to Bi/CN electronic effects as for the ν_{CO} spectra[14]), the survival of the E-dependent ν_{CN} feature suggests strongly that it is associated primarily with atop (or near-atop) Pt(111)–CN coordination.

Armed with this spectroscopic information on the likely surface binding geometry, we are in an advantageous position to interpret corresponding in-situ STM data for the Pt(111)/CN system. Figure 3 shows a typical STM image of a 25 nm square region of a Pt(111) terrace with a CN^- adlayer (dosed at −0.4 V) obtained at −0.4 V in 0.1 M $NaClO_4$ (pH 10.5). The pattern consists of clearly discerned hexagonally packed arrays, each containing a central spot surrounded by six slightly less intense "satellites." The row direction of these clusters was ascertained to lie essentially midway between those of the substrate Pt atoms. This deduction followed both from the (occasional) observation of substrate images for clean Pt(111), together with the known x-y orientation of the Pt(111) crystal in the STM base, yielding Pt rows rotated counterclockwise by 14° to the x-coordinate. The distance between neighboring clusters, 0.95 (±0.05) nm, is consistent with a $2\sqrt{3}$ side to the unit cell, yielding the adlayer symmetry $(2\sqrt{3} \times 2\sqrt{3})R30°$. A coverage of 7/12 is deduced by presuming that each spot (i.e. tunneling maximum) marks a single CN moiety.

The final deduction of the real-space adlayer structure follows from the above observation of predominant atop coordination. The most probable structure is shown in ball-model form in Fig. 4. This places the central CN group in each imaged cluster in a symmetric atop site, with the six "satellite" CN's occupying near-atop positions on the nearest neighbor Pt atoms. The latter designation is in harmony with the observed angular positions of the STM satellite spots. While locating the precise adsorbate geometry is complicated by probable electronic effects with the resulting tilted CN's, the occurrence of such near-atop binding is supported by its prediction[15] and observation[4,6,16] for compressed CO adlayers on Pt(111) and Rh(111). While slightly lower ν_{CN} frequencies are anticipated for near-atop compared with symmetry atop sites by analogy with CO adsorption, the frequency differences may well be small. Furthermore, a

substantial portion of the infrared absorption should be lost by intensity transfer to the nearby symmetric atop ν_{CN} band[4,15].

Essentially the same adlayer pattern is observed for cyanide dosing potentials, E_{dos}, between -0.6 and -0.3 V, over a wider range of applied potentials in the STM cell. For higher E_{dos} values, especially above -0.2 V, few ordered adlayer domains were observed; however, large ordered domains of the ($2\sqrt{3}$ × $2\sqrt{3}$) structure appear within a few minutes if the cell potential is altered to -0.5 V, which remain even if the potential is readjusted to values up to 0 V. Below -0.5 V, slow CN^- desorption occurs yielding a metastable (2 × 2) structure en route to largely disordered patterns.

Following the observation of such ordered adlayer structures for Pt(111)/CN, a similar investigation was made into the Pt(100)/CN system. This was prompted partly by the observation of a higher-frequency (2145-2165 cm^{-1}) band in the PDIR spectra, in addition to a feature at 2090-2120 cm^{-1} which appears to be similar to, if somewhat broader than, the single bipolar feature seen on Pt(111) [cf ref. 10]. As shown in Fig. 2B, the presence of a saturated predosed Bi adlayer removes selectively this higher-frequency component, suggesting that it is associated with a multifold or related binding site. Interestingly, STM images acquired for CN-covered Pt(100) surfaces, or for other adsorbates (eg CO, S^{2-}) dosed following the surface annealing procedure, display arrays of small (ca 3-5 nm) terrace domains, these being separated from each other by monoatomic steps running in various directions [17]. While the origin of the microscopic surface restructuring so to yield somewhat disordered surfaces is unclear [17], it is quite likely that the additional higher-frequency ν_{CN} feature is associated with adsorbate binding at step sites. This possibility is also consistent with the suggestion[10] that this vibrational feature arises from a $Pt(CN)_2$ or related "surface complex" associated with Pt(100) surface disordering.

The $(2\sqrt{3} \times 2\sqrt{3})R30°$ adlayer symmetry observed here for Pt(111)/CN is the same as that deduced from ex-situ LEED measurements [7,8]. Significantly, however, the *complete* real-space structure as deduced here by in-situ STM/IRAS differs from those suggested on the basis of the LEED data, although only the unit cell symmetry is extractable from the latter in the absence of a detailed electron energy-dependent diffraction analysis. The present less uniform adlayer structure, with CN occupying atop and adjacent near-atop sites, can be anticipated in view of the prevailing characteristic of CN for σ-donation rather than π-acceptor binding to metals [18]. The apparent "gaps" between the hexagonal CN clusters in the present adlayer structure (Fig 4) may well be occupied by solvent molecules and/or coadsorbed cations; the latter is plausible in view of the specific involvement of cations in the Pt(111)/CN double-layer structure as deduced from detailed ex-situ measurements [7,8].

In conclusion, the present study provides further evidence of the virtues of combined STM/IRAS measurements for deducing atomic-level structural information for simple molecular adlayers at in-situ metal-solution interfaces. While limited by several factors, including the need for immobility as well as local adlayer order along with the occurrence of suitably diagnostic vibrational features, this tactic can provide a degree of real-space structural insight which is unprecedented for electrochemical systems.

Acknowledgments

Carol Korzeniewski kindly shared with us her infrared data (ref. 10) prior to publication. C.S. gratefully acknowledges a Feodor Lynen Fellowship from the Alexander von Humboldt Foundation of Germany. This work is also supported in part by the U.S. National Science Foundation and the Office of Naval Research.

References

1) A.T. Hubbard, Chem. Rev., 88 (1988), 633.

2) M.J. Weaver and X. Gao, Ann. Rev. Phys. Chem., 44 (1993), 459.

3) For example: J.P. Biberian and M.A. Van Hove, Surf. Sci., 138 (1984), 361; 118 (1982), 443; B. Voigtländer, D. Bruchmann, S. Lehwald, and H. Ibach, Surf. Sci., 225 (1990), 151.

4) S-L. Yau, X. Gao, S-C. Chang, B.C. Schardt, and M.J. Weaver, J. Am. Chem. Soc., 113 (1991), 6049.

5) X. Gao, S-C. Chang, X. Jiang, A. Hamelin, and M.J. Weaver, J. Vac. Sci. Tech., A10 (1992), 2972.

6) I. Villegas and M.J. Weaver, in preparation.

7) S.D. Rosasco, J.L. Stickney, G.N. Salaita, D.G. Frank, J.Y. Katekaru, B.C. Schardt, M.P. Soriaga, D.A. Stern, and A.T. Hubbard, J. Electroanal. Chem., 188 (1985), 95.

8) D.G. Frank, J.Y. Katekaru, S.D. Rosasco, G.N. Salaita, B.C. Schardt, M.P. Soriaga, D.A. Stern, J.L. Stickney, and A.T. Hubbard, Langmuir, 1 (1985) 587.

9) V.B. Paulissen and C. Korzeniewski, J. Phys. Chem., 96 (1992), 4563.

10) C.S. Kim and C. Korzeniewski, J. Phys. Chem., 97 (1993), 9784.

11) D. Zurawski, L. Rice, M. Hourani, and A. Wieckowski, J. Electroanal. Chem., 230 (1987), 221.

12) S-C. Chang and M.J. Weaver, J. Chem. Phys., 92 (1990), 4582.

13) X. Gao, G.J. Edens, A. Hamelin, and M.J. Weaver, Surf. Sci., 296 (1993), 333.

14) S-C. Chang and M. J. Weaver, Surf. Sci., 241 (1991), 11.

15) B.N.J. Persson, M. Tüshaus, and A.M. Bradshaw, J. Chem. Phys., 92 (1990), 5034.

16) M.A. Van Hove, R.J. Koestner, J.C. Frost, and G.A. Somorjai, Surf. Sci., 129 (1983), 482.

17) I. Villegas and M.J. Weaver, in preparation.

18) K. Nakamoto in "Infrared and Raman Spectra of Inorganic and Coordination Compounds", Wiley, New York, 4th Edition, 1986, page 272.

Figure Captions

Figure 1

Representative potential-difference infrared (PDIR) spectra for a cyanide adlayer on Pt(111) in 0.1 M $NaClO_4$ (pH 10.5) formed by prior dosing in a CN^--containing solution at -0.6 V vs. SCE. Spectral "reference" potential is -0.5 V; sample potentials are as indicated (see text for further details).

Figure 2

A) PDIR spectra for CN^- adlayer on Pt(111) from -0.3 V to 0.1 V in the absence and presence of predosed saturated Bi adlayer, as indicated (see text).

B) As for A, but for CN^- adlayer on Pt(100).

Figure 3

Typical mildly filtered STM image of a 5 nm square region of the $(2\sqrt{3} \times 2\sqrt{3})R30°$-7CN adlayer on Pt(111) in 0.1 M $NaClO_4$ (pH 10.5) at -0.4 V vs. SCE. Substrate-tip bias potential = -100 mV; tunneling current = 10 nA.

Figure 4

Ball model of the proposed $(2\sqrt{3} \times 2\sqrt{3})R30°$-7CN adlayer on Pt(111). Smaller semifilled circles denote positions of CN^- adsorbate.

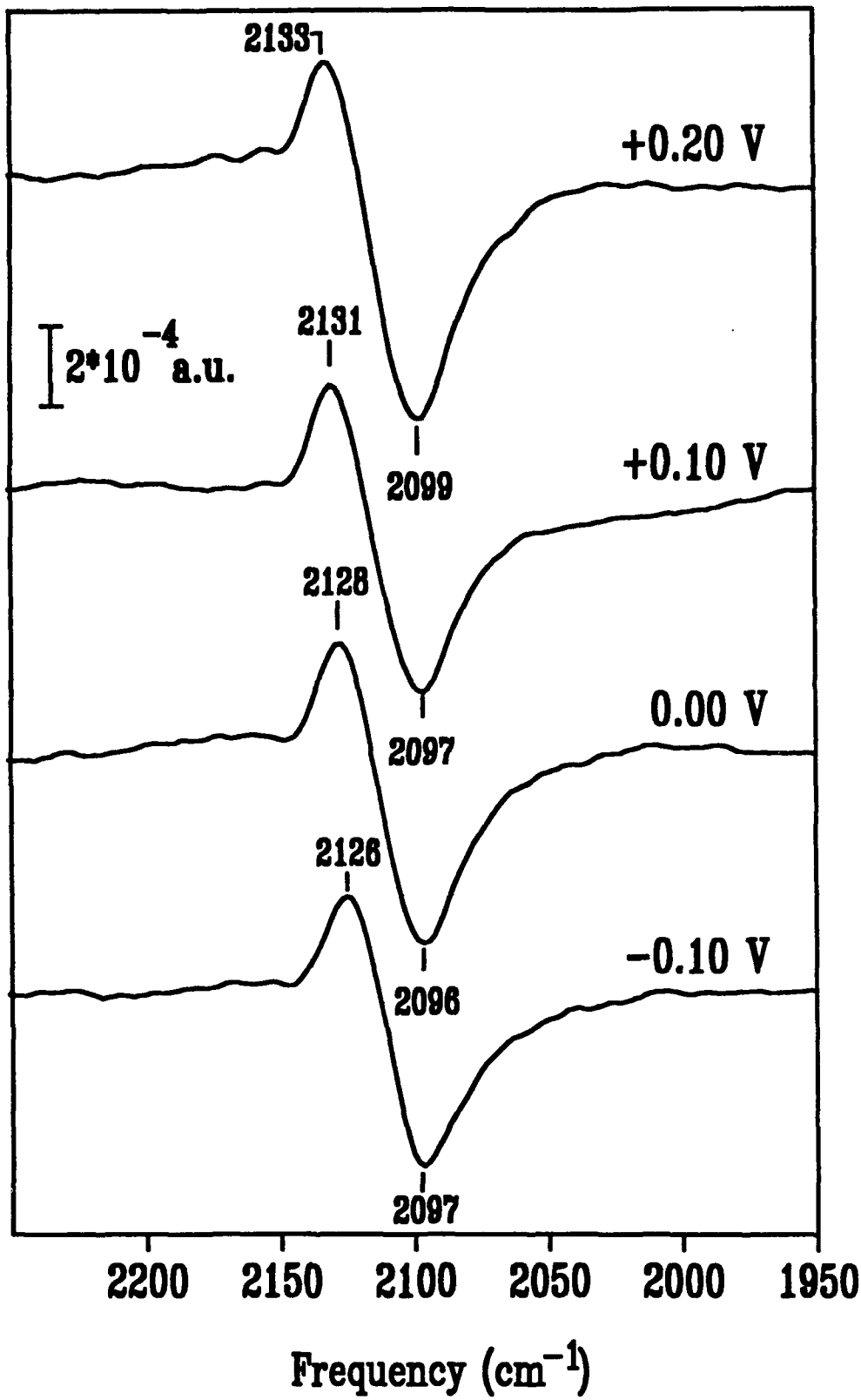
2133
+0.20 V
2131
2*10 -4 a.u.
2099
+0.10 V
2128
2097
0.00 V
2126
2096
-0.10 V
2097
2200
2150
2100
2050
2000
1950
Frequency (cm-1)

FIG1

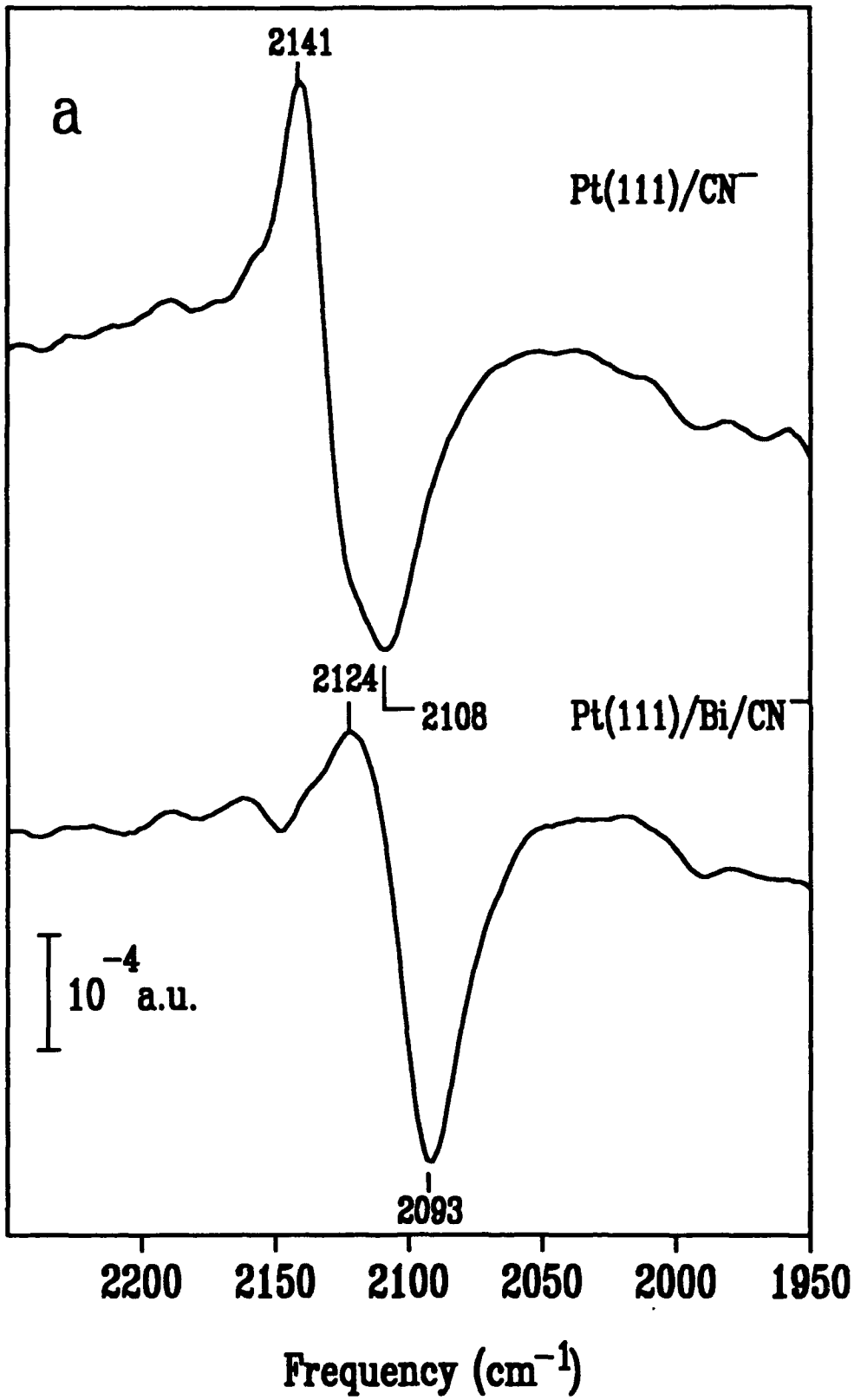
2141
a
Pt(111)/CN⁻
2124
2108
Pt(111)/Bi/CN⁻
10⁻⁴ a.u.
2093
2200
2150
2100
2050
2000
1950
Frequency (cm⁻¹)

FIG 2A

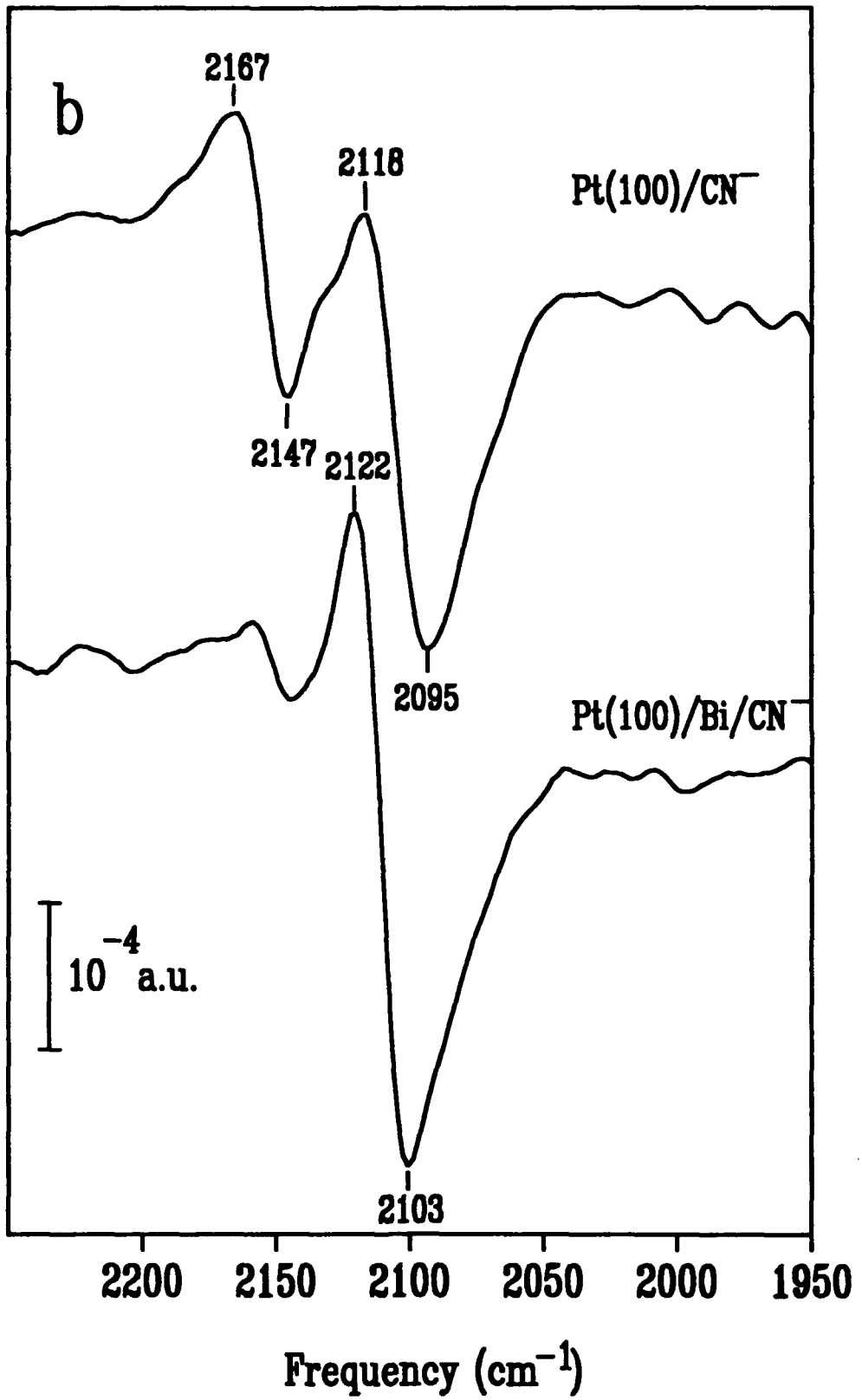
b
2167
2118
Pt(100)/CN⁻
2147
2122
2095
Pt(100)/Bi/CN⁻
10⁻⁴ a.u.
2103
2200
2150
2100
2050
2000
1950
Frequency (cm⁻¹)

FIG 2B

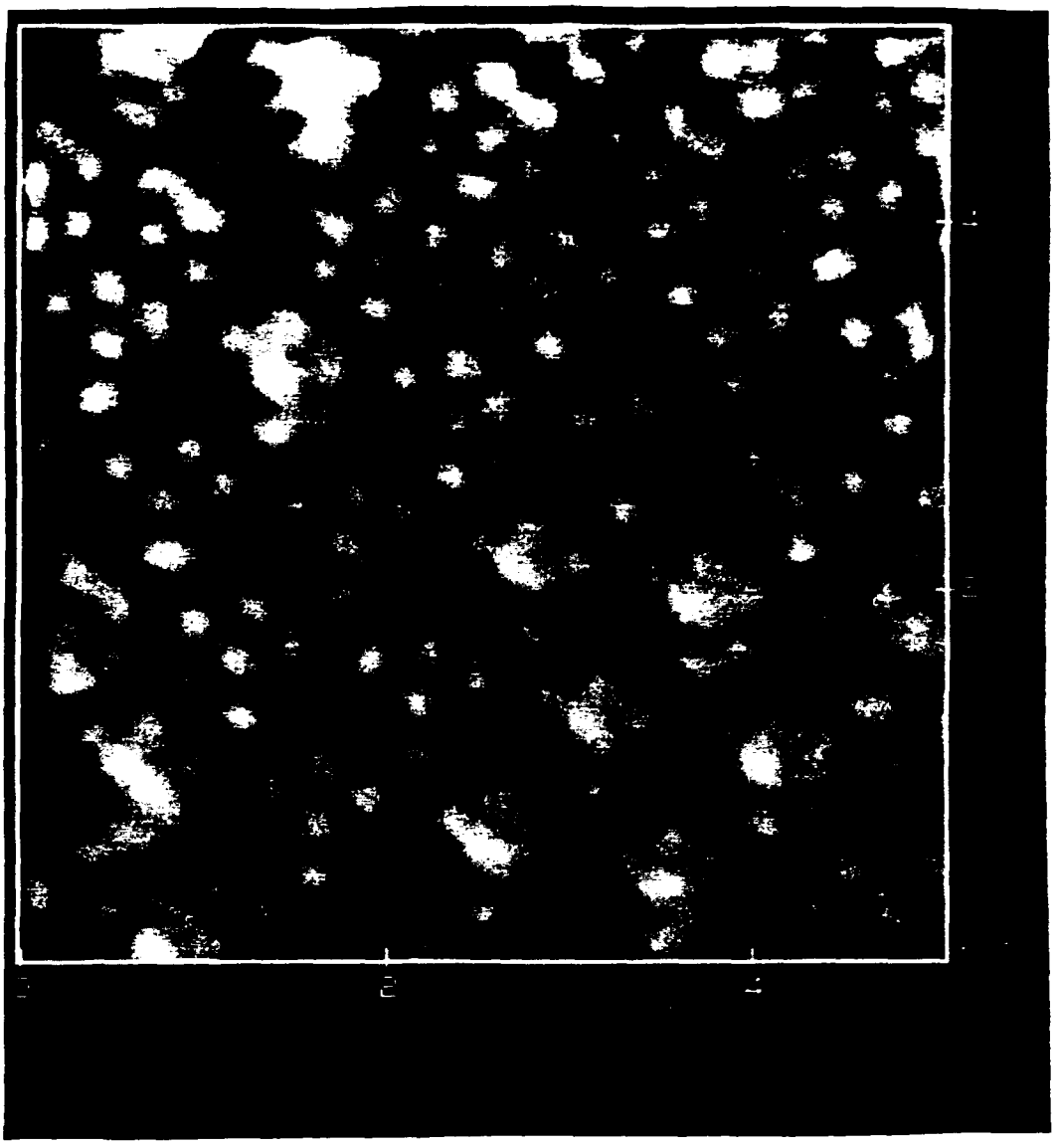

FIG 3

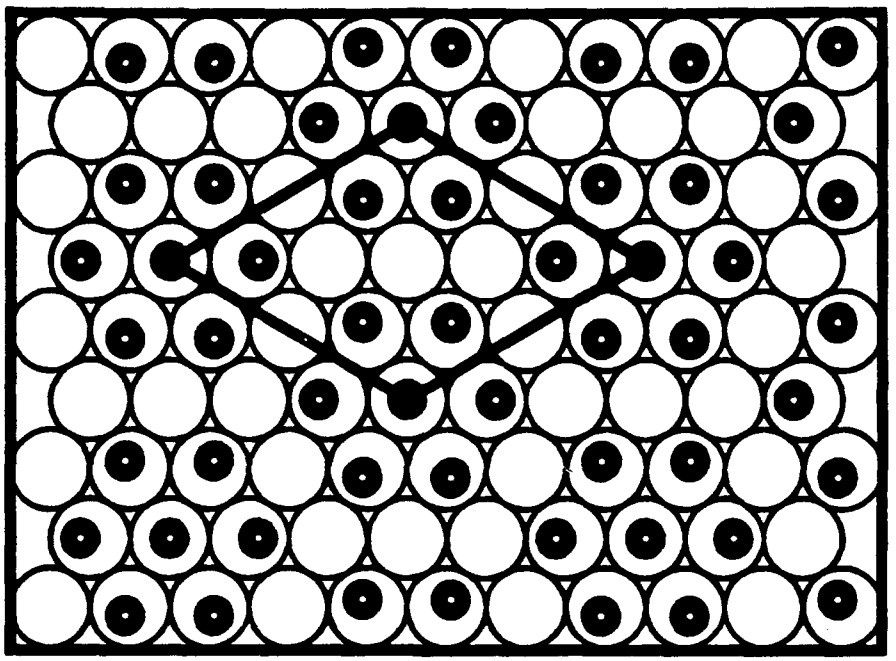

FIG 4